Available online at www.sciencedirect.com
ScienceDirect
Journal of Hazardous Materials 155 (2008) 449–458
Journal of Hazardous Materials
www.elsevier.com/locate/jhazmat

Liquid–solid phase countercurrent multi-stage adsorption process for using the Langmuir equation

Feng-Chin Wu [a], Ru-Ling Tseng [b,*]

[a] *Department of Chemical Engineering, National United University, Miao-Li 360, Taiwan*
[b] *Department of Safety, Health and Environmental Engineering, National United University, No.1, Lien Da, Kung-Ching Li, Miao-Li 360, Taiwan*

Received 11 October 2007; received in revised form 22 November 2007; accepted 22 November 2007
Available online 7 January 2008

Abstract

Mass balance and the Langmuir equation were used to deduct the countercurrent multi-stage adsorption process. The relationships between the Langmuir parameter ($K_L y_i$) and the required amounts of adsorbent in countercurrent two-, three- and infinite-stage processes were obtained to find the optimum number of stages as well as the reduction in the adsorbent consumption of the countercurrent multi-stage process of an adsorption system. Pistachio shell activated carbons with BET surface areas of 1013, 1398, and 1919 m^2/g were obtained by KOH activation with CO_2 gasification at gasification times of 0, 10, and 30 min. The isotherm adsorption of four adsorbates were investigated and analyzed with the Langmuir equation. The activated carbons studied in this work show compared with other published literatures, the $K_L y_i$ and q_{mon} values in this work showed excellent adsorption performance. The amount of activated carbon for a countercurrent two- and single stage adsorption operation was calculated, a saving of 66–87% adsorbent was obtained. A simple countercurrent two-stage adsorption system was designed for use in engineering applications.

Keywords: Activated carbon; Countercurrent multi-stage; Adsorption process; Langmuir equation; Equilibrium-stage

1. Introduction

Countercurrent multi-stages are widely applied in separating processes in chemical engineering, such as distillation, liquid extraction, gas absorption or stripping, and also for improving efficiency of separation and purification. However, they are rarely applied to adsorption. In 1976, deRosset et al. submitted *p*-xylene purification with continuous countercurrent adsorptive separations [1]. It was a complicated system with multiple rotating tubes which was hard to operate; not suitable for wide application. Vanderschuren used multi-stage fluidized bed absorbers to remove the moisture from air. However, the steady operation for the descending solid particles in multiple plate columns is hardy achieved. This was not an easy process [2]. Ruthven theoretically analyzed continuous countercurrent adsorbers, but there was no practical application [3]. Recently, pressure swing adsorption (PSA) was developed and effectively used in gas separation, the best example of countercurrent multi-stages applied in an adsorption system. In theory, adsorption operation in a solution using countercurrent multi-stages can largely reduce adsorbent consumption. Ultimately however, no suitable adsorption process has been submitted so far.

In this study, mass balance was used to deduce the amounts of adsorbent for various countercurrent multi-stages, and to determine the optimum number of stages for adsorbent reduction. Pistachio shell activated carbons were prepared using KOH activation with CO_2 gasification. The isotherm equilibrium adsorptions of two dyes and two phenols were investigated. The results were used for calculating reductions in adsorbent consumption in various countercurrent multi-stages. Furthermore, a simple countercurrent multi-stage adsorption system was designed to be used in engineering applications.

2. Materials and method

2.1. Preparation of the activated carbon

Activated carbon was prepared from Pistachio shells with carbonization and activation; a two-step process. During carbonization, the oven temperature was kept at 450 °C for 1.5 h

* Corresponding author. Tel.: +886 37 381775; fax: +886 37 333187.
E-mail address: trl@nuu.edu.tw (R.-L. Tseng).

0304-3894/$ – see front matter © 2007 Published by Elsevier B.V.
doi:10.1016/j.jhazmat.2007.11.086

while nitrogen gas was flowed into the oven at a rate of 3 dm^3/min.

During activation, a mixture of water/KOH/char with a ratio of 1/1/1 by mass was placed in a sealed ceramic oven, heated at a rate of 10 °C/min to 780 °C, and kept at this temperature for 1 h while nitrogen gas was flowed into the oven at a rate of 3 dm^3/min. Then, the nitrogen gas was shut off and CO_2 started to flow into the oven at a rate of 2 dm^3/min. The samples were classified according to the CO_2 gasification times: 0, 10, and 30 min called PS100, PS110, and PS130, respectively. According to literature, in applications of activated carbon in electric double-layer capacitors, KOH carbon activation followed by a suitable time of CO_2 gasification performs excellently [4].

2.2. Procedures for adsorption experiments

A commercial-grade acid dye, Acid Blue 74, (AB74) (Bayer), was used. The methylene blue (MB, M_W (molecular weight) = 284.3 g/mol), phenol (M_W = 94 g/mol), and 4-chlorophenol (4-CP, M_W = 128.5 g/mol) were analytical reagent grade. The procedures for the adsorption equilibrium experiments were the same as in a previous study [5].

3. Theory

3.1. Graphical method for the countercurrent multi-stage adsorption system

In countercurrent multi-stage adsorption there are J stirred vessels in series; the mode of operation is as shown in Fig. 1. The influent solution with mass m_{yi} and concentration y_i enters the Jth stirred vessel, makes sufficient contact with the adsorbent with mass m_{xJ-1} and solute concentration x_{J-1} and is separated after equilibrium is reached. Then, the separated adsorbent with mass m_{xJ} and solute concentration x_J leaves the adsorption process and enters the $J-1$ stirred vessel, comes into contact with the adsorbent with mass m_{xJ-1} and solute concentration x_{J-1} is separated, and so on. The concentration of the separated solution from the first stage after equilibrium is y_1, i.e., the last solution concentration is y_f and the adsorbent with mass m_{x0} and solute concentration x_0 enters this stage (the first stage).

Suppose the mass of the solution is the same in all stages, then

$$m_y = m_{yi} = m_{y1} = m_{y2} = \cdots m_{yJ-1} = m_{yf} \quad (1)$$

and the mass of adsorbent is the same in all stages, then

$$m_x = m_{xi} = m_{x0} = m_{x1} = m_{x2} = \cdots = m_{xJ-1} = m_{xJ} \quad (2)$$

Make the mass balance on any stage of the countercurrent multi-stage adsorption process as shown in Fig. 2, then

$$m_y(y - y_f) = m_x(x - x_0) \quad (3)$$

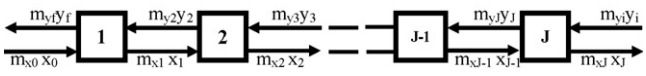

Fig. 1. Countercurrent multi-stage adsorption process.

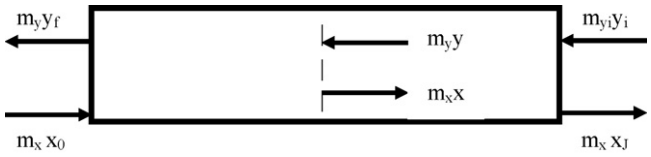

Fig. 2. Mass balance of the countercurrent multi-stage adsorption process.

$$y = \left(\frac{m_y}{m_x}\right)x + \left[y_f - \left(\frac{m_y}{m_x}\right)x_0\right] \quad (4)$$

Eq. (4) is the operating line equation of the countercurrent multi-stage adsorption process. The operating line is a straight line with constant slope (m_y/m_x) and y-intercept [$y_f - (m_y/m_x)x_0$].

Suppose adsorption equilibrium is described with the Langmuir isotherm equation, then

$$q_e = \frac{K_L q_{mon} C_e}{1 + K_L C_e} \quad (5)$$

If C_e (g/m^3), solute concentration of the solution, is substituted with y_J, and q_e (g/kg), solute concentration (adsorption amount) of the solid phase, is substituted with x_J/ρ, where ρ is the adsorbent mass per unit solution volume kg/m^3. Then, after Eq. (5) is rewritten, the isotherm equilibrium of the Jth stage is

$$\frac{x_j}{\rho} = \frac{K_L q_{mon} y_J}{1 + K_L y_J} \quad (6)$$

The solute equilibrium relationship between solid phase and liquid phase of adsorption described with Eq. (6) is called isotherm curve.

According to the operating line of Eq. (4) and the isotherm curve of Eq. (6), the countercurrent multi-stage adsorption operation is graphically shown in Fig. 3. The two ends of the operating line are, respectively (x_0, y_f) and (x_J, y_i). The ideal number of stages of the countercurrent multi-stage adsorption can be obtained from Fig. 3. The procedures are as follows: start at point (x_0, y_f), draw horizontal line which intersects isotherm curve at point (x_1, y_f). Then, a vertical line is drawn from this

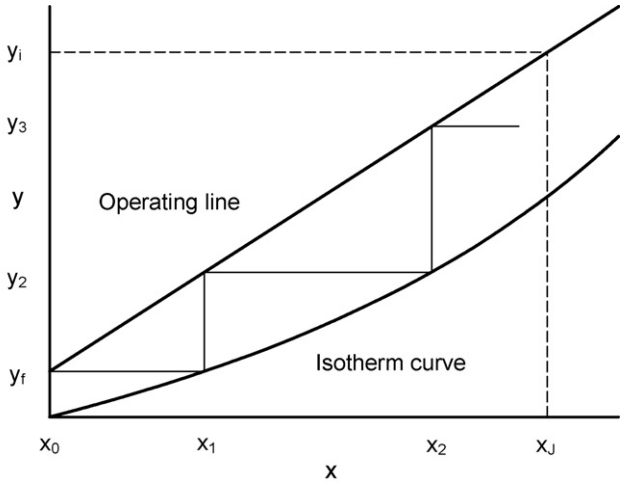

Fig. 3. Ideal stages of the countercurrent multi-stage process.

point intersecting the operating line at point (x_1, y_2). This completes an ideal stage, and so on. After point (x_f, y_i) is passed over, the obtained drawn stage number is the required ideal stage number of countercurrent multi-stage adsorption.

There is a direct relationship between the ideal stage number and the slope (m_y/m_x) of the operating line. When one end (x_0, y_f) of the operating line is fixed, and the slope (m_y/m_x) is decreased, the other end (x_f, y_i) of the operating line moves right and toward the isotherm curve, and ideal stage number increases. If (m_y/m_x) keeps decreasing the operating line intersects the isotherm curve at point (x_f, y_i). At this stage, the ideal stage number is infinite and its adsorbent amount is the minimum. This is the minimum adsorbent mass ($m_{y,\min}$).

3.2. Adsorbent consumption for the countercurrent multi-stage adsorption system

A single stage adsorption operation is shown in Fig. 4(a). The operating line equation of Eq. (4) can be rewritten as

$$y_i = \left(\frac{m_x}{m_y}\right)_s x_f + \left[y_f - \left(\frac{m_x}{m_y}\right) x_0\right] \tag{7}$$

and rearranged as

$$\left(\frac{m_x}{m_y}\right)_s = \frac{y_i - y_f}{x_f - x_0} \tag{8}$$

If fresh adsorbent is used, then $x_0 = 0$. When the isotherm curve of Eq. (6) is inserted into Eq. (8), then

$$\left(\frac{m_x}{m_y}\right)_s = \frac{y_i - y_f}{\rho(K_L q_{mon} y_f)/(1 + K_L y_f)} \tag{9}$$

If the Langmuir constant is known, mass ratio $(m_x/m_y)_s$ of adsorbent to solvent for a single stage can be calculated from Eq. (9).

Fig. 4(b) gives the analysis for the countercurrent two-stage adsorption operation. Because the operating line is straight, the slope of all stages is the same and can be expressed as

$$\left(\frac{m_x}{m_y}\right)_d = \frac{y_2 - y_f}{x_1 - x_0} = \frac{y_i - y_2}{x_2 - x_1} = \frac{y_i - y_f}{x_2 - x_0} \tag{10}$$

$$\left(\frac{m_x}{m_y}\right)_d = \frac{y_2 - y_f}{\rho(K_L q_{mon} y_f)/(1 + K_L y_f)} \tag{11}$$

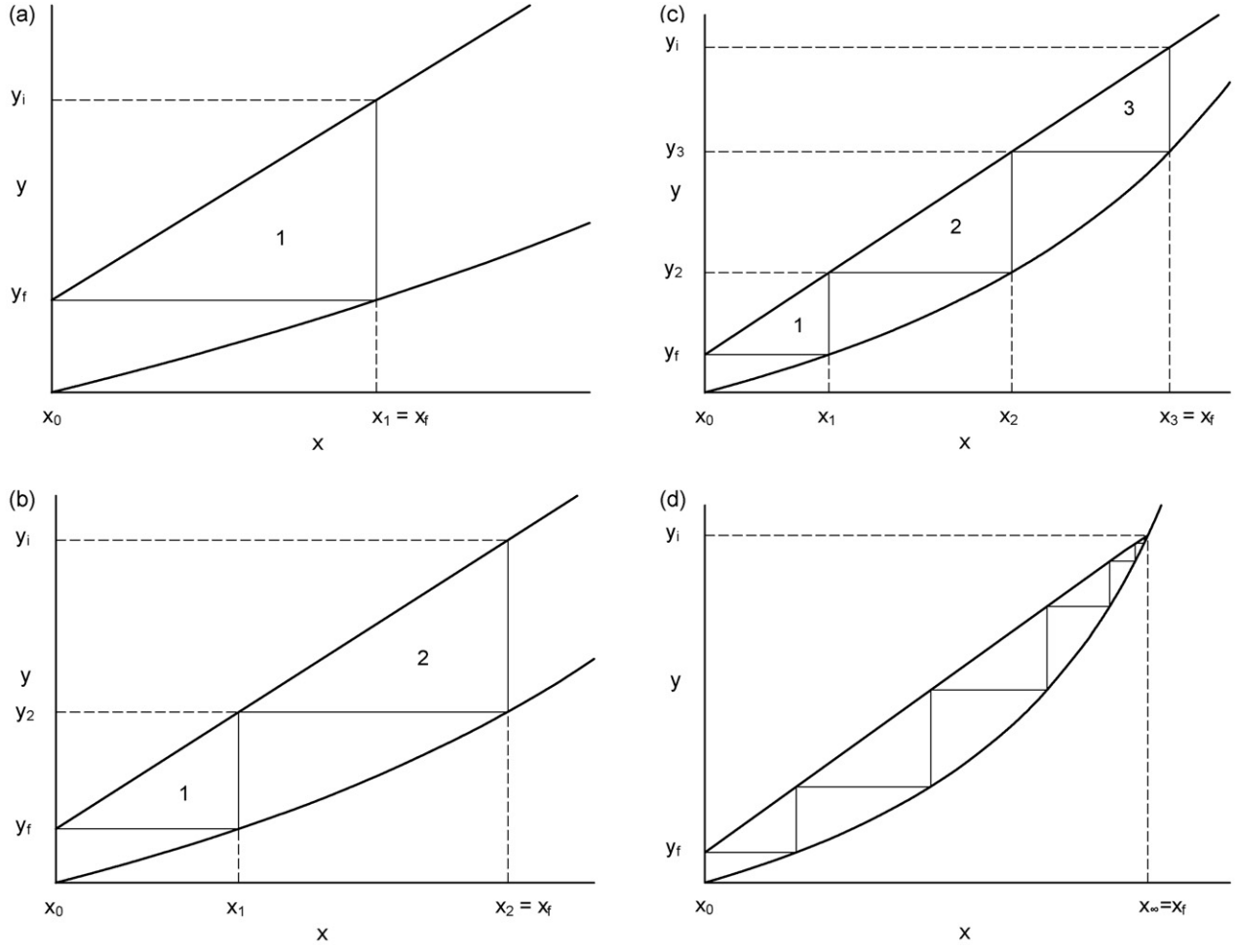

Fig. 4. (a) Ideal stages of the single stage process. (b) Ideal stages of the countercurrent two-stage process. (c) Ideal stages of the countercurrent three-stage process. (d) Ideal stages of the countercurrent ∞-stage process.

If $x_0 = 0$, and the isotherm curve is expressed with the Langmuir equation, then

$$\frac{y_2 - y_f}{\rho(K_L q_{mon} y_f)/(1 + K_L y_f)} = \frac{y_i - y_f}{\rho(K_L q_{mon} y_2)/(1 + K_L y_2)} \quad (12)$$

After rearranging

$$\frac{y_2 - y_f}{y_i - y_f} = \frac{y_f}{y_2}\left[\frac{1 + K_L y_2}{1 + K_L y_f}\right] \quad (13)$$

When y_i, y_f, and the Langmuir constant are known, the middle concentration y_2 of the two countercurrent stages can be calculated from Eq. (13).

The adsorbent mass ratio of the countercurrent two-stage to the single stage from the following Eq. (14), obtained by dividing Eq. (11) by Eq. (9), is:

$$\left(\frac{m_x}{m_y}\right)_s \Big/ \left(\frac{m_x}{m_y}\right)_d = \frac{y_i - y_f}{y_2 - y_f} = \frac{m_{xs}}{m_{xd}} \quad (14)$$

Where m_{xs}/m_{xd} is the adsorbent mass ratio of the countercurrent two-stage to single stage.

Countercurrent three-stage adsorption operation is shown in Fig. 4(c). The operating line is a straight line, so, the slope is the same of all stages, and

$$\left(\frac{m_x}{m_y}\right)_t = \frac{y_2 - y_f}{x_1 - x_0} = \frac{y_3 - y_f}{x_2 - x_0} = \frac{y_i - y_f}{x_3 - x_0} \quad (15)$$

$$\left(\frac{m_x}{m_y}\right)_t = \frac{y_2 - y_f}{\rho(K_L q_{mon} y_f)/(1 + K_L y_f)} \quad (16)$$

If $x_0 = 0$, then

$$\frac{y_2 - y_f}{x_1} = \frac{y_3 - y_f}{x_2} \quad (17)$$

$$\frac{y_2 - y_f}{x_1} = \frac{y_i - y_f}{x_3} \quad (18)$$

When the isotherm curve follows the Langmuir equation, Eqs. (17) and (18) can be rearranged, respectively, as

$$\frac{y_2 - y_f}{y_3 - y_f} = \left(\frac{y_f}{y_2}\right)\left[\frac{(1 + K_L y_2)}{(1 + K_L y_f)}\right] \quad (19)$$

$$\frac{(y_2 - y_f)}{(y_i - y_f)} = \left(\frac{y_f}{y_3}\right)\left[\frac{(1 + K_L y_3)}{(1 + K_L y_f)}\right] \quad (20)$$

When y_i, y_f, and the Langmuir constant are known, the middle concentration (y_2 and y_3) of countercurrent three-stages one can be obtained by simultaneously solving Eqs. (19) and (20). Adsorbent mass ratio of countercurrent three-stage one to single stage one can be obtained from the following Eq. (21), which is obtained by dividing Eq. (16) by Eq. (9).

$$\frac{(m_x/m_y)_s}{(m_x/m_y)_t} = \frac{y_i - y_f}{y_2 - y_f} = \frac{m_{xs}}{m_{xt}} \quad (21)$$

where m_{xs}/m_{xt} is the adsorbent mass ratio of a countercurrent three-stage one to a single stage one.

Fig. 4(d) shows the countercurrent infinite-stage adsorption operation. The slope of its operating line is

$$\left(\frac{m_x}{m_y}\right)_\infty = \frac{y_i - y_f}{x_\infty - x_0} \quad (22)$$

When $x_0 = 0$, and Eq. (10) is divided by Eq. (22) the adsorbent mass ratio of the countercurrent infinite-stage one to single stage one is

$$\left(\frac{m_x}{m_y}\right)_s \Big/ \left(\frac{m_x}{m_y}\right)_\infty = \frac{(y_i - y_f)/x_f}{(y_i - y_f)/x_\infty} = \frac{x_\infty}{x_f} \quad (23)$$

Let isotherm curve be expressed with Langmuir equation, then

$$\frac{m_{xs}}{m_{y\infty}} = \left(\frac{y_i}{y_f}\right)\left[\frac{1 + (K_L y_f)}{(1 + K_L y_i)}\right] \quad (24)$$

The relationships between the required adsorbent amounts of countercurrent two-, three- and infinite-stage processes and Langmuir parameter ($K_L y_i$) were obtained to determine the optimum number of stages and the adsorbent consumption reduction of the countercurrent multi-stage process for a specific adsorption system.

Suppose concentration ratio (y_f/y_i) of influent to effluent is 0.01 and $K_L y_i$ value is known, then the middle concentration ratio (y_j/y_i) of the countercurrent two-stage one to the three-stage one can be obtained from Eqs. (13), (17) and (18), and adsorbent consumptions (m_{xs}/m_{xd} and m_{xs}/m_{xt}) of the two- and three-stage ones can be obtained from Eqs. (14) and (21), and the adsorbent consumption of the countercurrent infinite-stage adsorption operation can be obtained from Eq. (24). Table 1 lists values of m_{xs}/m_{xd}, m_{xs}/m_{xt}, and $m_{xs}/m_{x\infty}$. When the $K_L y_i$ value of the adsorption process is 1, the adsorbent consumption of the single stage one is 10 times that of the countercurrent two-stage one, 21.13 times that of the countercurrent three-stage one, or 50.5 times that of the countercurrent ∞-stage one. Increasing the number of stages significantly saves on adsorbent consumption in countercurrent multi-stage adsorption operations.

When the $K_L y_i$ value of the adsorption process is 10, the adsorbent consumption of the single stage one is, respectively, 9.48 and 10.0 times that of the countercurrent three-stage and ∞-stage ones, revealing a marginal saving of adsorbent consumption for more than three-stages. Thus, three is the optimum number of stages. When the $K_L y_i$ value of adsorbent is 33.3, the adsorbent consumption of the single stage one is, respectively, 3.61 and 3.88 times that of the countercurrent two-stage

Table 1
Ratio of adsorbent consumption of a single-stage to that of a countercurrent multi-stage process (at $y_f/y_i = 0.01$)

$K_L y_i$	m_{xs}/m_{xd}	m_{xs}/m_{xt}	$m_{xs}/m_{x\infty}$	Optimum stage number
1	10.00	21.13	50.50	>3
10	6.73	9.48	10.00	3
33.3	3.61	3.88	3.89	2
100	1.96	1.98	1.98	2
1000	1.099	1.099	1.099	1

and three-stage ones. The three-stage one is of little benefit in the saving of adsorbent consumption, thus, two is the optimum number of stages.

The optimum numbers of stages are listed in the last column of Table 1. It shows that the optimum number of stages is in reverse order to the $K_L y_i$ value. When the $K_L y_i$ value is 10^3, the corresponding optimum number of stage is 1; when the $K_L y_i$ value is 10^2, the corresponding optimum number of stages is 2; when the $K_L y_i$ value is 10^1, the corresponding optimum number of stages is 3; and when the $K_L y_i$ value is 10^0, the corresponding optimum number of stages is more than 3.

4. Results and discussion

4.1. Properties of the activated carbons

The activated carbons in this study were denoted according to the CO_2 gasification time of 0, 10, and 30 min as PS100, PS110, and PS130. Table 2 lists the BET surface area related data (S_p, S_{micro}/S_p, V_{pore}, V_{micro}/V_{pore}, and D_p) obtained from 77 K N_2 isotherm adsorption with a sorptiometer. Of these, the surface area (S_p) and pore volume (V_{pore}) increased with increased CO_2 gasification time; the micropore area ratio (S_{micro}/S_p) and micropore volume ratio (V_{micro}/V_{pore}) significantly dropped with the CO_2 gasification time from 10 to 30 min, meaning higher ratio of mesopores developing in the pores; the average pore diameter (D_p) stayed at 2.4 nm, meaning, according to the definition of D_p being 4 V_{pore}/S_p, that the values of V_{pore} and S_p increased equally in proportion with the increased CO_2 gasification time.

Fig. 5(a)–(c) has 2000× magnified SEM photos of the activated carbons. Fig. 5(a) shows PSChar: carbonized char from Pistachio shells. The cut face of a broken particle is flat and complete. PS100 in Fig. 5(b) kept the original of flat, completely cut surface. This phenomenon proved again the finding of the previous study [6], namely that KOH activation causes homogeneous etching in the interior of a material. Fig. 5(c) shows an up and down cut surface of PS130 caused by a CO_2 gasification time of 30 min.

Temperature programmed desorption (TPD) was used to analyze the chemical properties of the activated carbon surface. Inert gas (He) was flowed through the sample surfaces in temperature programmed desorption. Desorption began when the temperature of the sample rose. At lower temperatures (<550 °C) CO_2 was desorbed because of the presence of anhydrides, lactones, and carboxyl. The desorption of CO occurred at higher temperatures (above 500 °C) because of the presence of quinine, hydroxyl, and carbonyl groups [7–9]. Thus, distribution of the oxygen-containing functional groups could be analyzed based on the TPD results. Fig. 6 shows the results of the TPD of the activated carbon studied in this work. The desorption of

Table 2
Physical properties of carbons derived from Pistachio shells with KOH plus CO_2 activation

Carbon	t_g[a] (min)	S_p (m^2/g)	S_{micro}/S_p	V_{pore} (cm^3/g)	V_{micro}/V_{pore}	D_p (nm)
PS100	0	1013	0.92	0.60	0.80	2.4
PS110	10	1398	0.92	0.84	0.82	2.4
PS130	30	1919	0.85	1.16	0.67	2.4

[a] CO_2 gasification time.

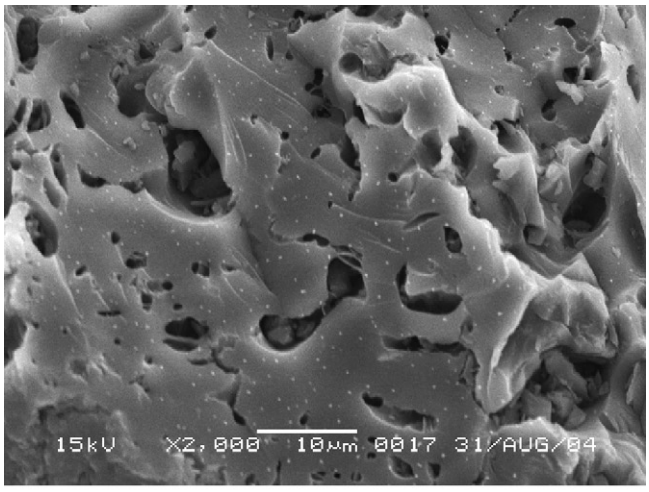

(a)

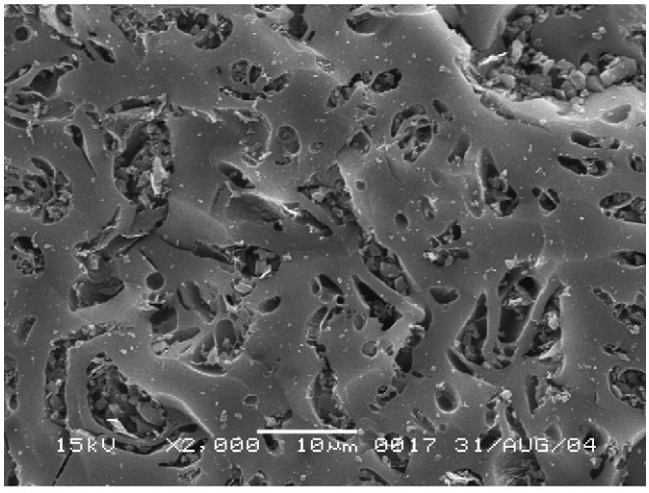

(b)

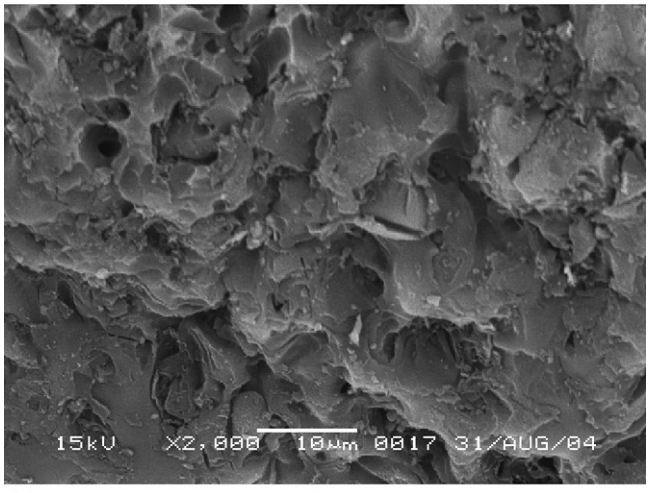

(c)

Fig. 5. SEM photos: (a) PSChar, (b) PS100, (c) PS130.

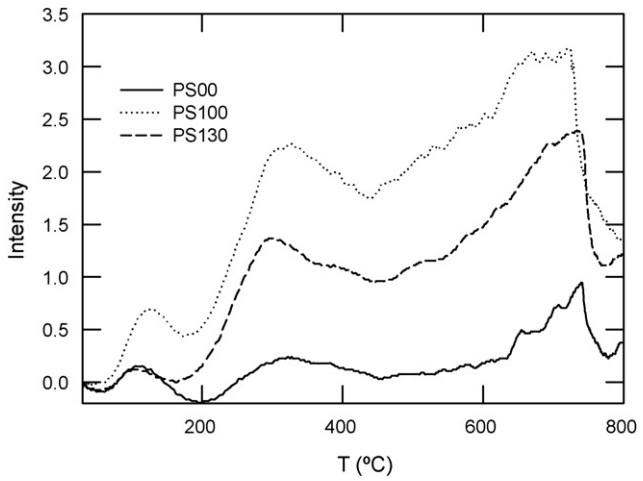

Fig. 6. Evolution profiles of CO_2 and CO by temperature programmed desorption (carbons are PS00 (–), PS100 (. . .), and PS130 (– –), respectively).

PS00 at lower temperatures (<550 °C) and at higher temperatures (>500 °C) was the least. The preparation was the same as that of the PS100 physical activation, only without KOH. The desorption of PS100 at both temperature ranges was the highest; that of PS130 was between the two. Fig. 6 shows that the homogeneity of KOH activation preserved more surface functional groups, while physical activation on the pore surface caused the loss of some surface functional groups; the effect of KOH activation with CO_2 gasification on functional groups was between the two, because it involved both physical and chemical processes.

4.2. Adsorption equilibrium and Langmuir isotherm equation

Two dyes (AB74 and MB) and two phenols (phenol and 4-CP) were used as adsorbates and PS100, PS110, and PS130, the activated carbons of different CO_2 gasification times, were used as adsorbents for the isotherm equilibrium adsorption study. The results are shown in Fig. 7(a)–(d) and will be discussed later. A Langmuir isotherm equation was used for analysis. The equation is as follows:

$$\frac{C_e}{q_e} = \frac{1}{K_L q_{mon}} + \left(\frac{1}{q_{mon}}\right) C_e \tag{25}$$

where q_{mon} is the amount of adsorption (in g/kg) corresponding to complete monolayer coverage and K_L is the Langmuir constant. If C_e/q_e is on the Y-axis and C_e is on the X-axis, the slope ($1/q_{mon}$) and intercept ($1/K_L q_{mon}$) can be obtained from the least number of squares, the correlation coefficient (r^2), and the separation factor (R_L). Table 3 lists the q_{mon}, K_L, r^2 and R_L values. The r^2 is between 0.989 and 1.000, implying a good equation fitting. Calculation values of the curves in Fig. 7 were obtained from calculating the Langmuir parameters listed in Table 3 revealing good agreement between calculated and experimental values.

The Langmuir equation constants of 28 adsorption systems of dyes on various activated carbons from literature have been collected in Table 4 to compare with the results from this work. The sequence is according to the $K_L y_i$ values. The top $K_L y_i$ val-

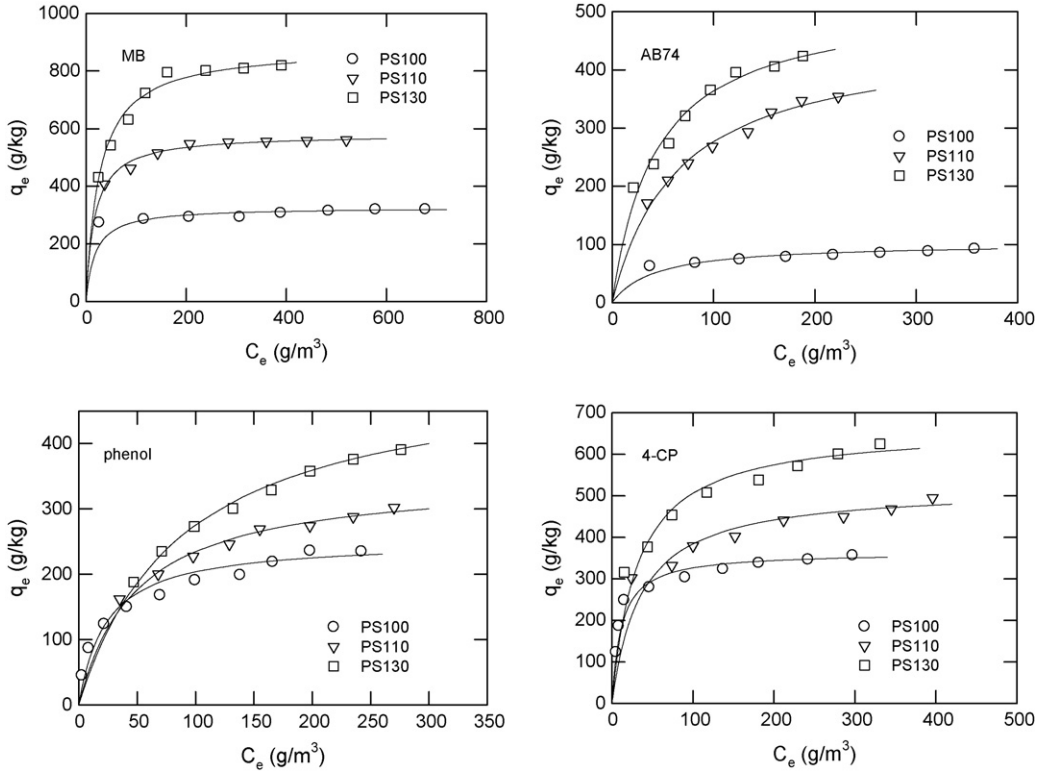

Fig. 7. Fitting of the Langmuir equation for the adsorption of dyes and phenols on the Pistachio shell activated carbons (a) MB, (b) AB74, (c) phenol, (d) 4-CP (carbons are PS100 (◯), PS110 (▽), and PS130 (□), respectively).

Table 3
Langmuir isotherm equation analysis of the adsorption system of various adsorbates on the activated carbons

Adsorbate	Carbon	r^2	q_{mon} (g/kg)	K_L (m^3/g)	R_L[a]
MB	PS100	0.998	327	0.0561	0.0218
	PS110	1.000	581	0.0583	0.0210
	PS130	0.999	883	0.0373	0.0325
AB74	PS100	0.992	102	0.0237	0.0954
	PS110	0.993	456	0.0154	0.0160
	PS130	0.992	521	0.0232	0.0974
Phenol	PS100	0.989	251	0.0428	0.0474
	PS110	0.996	349	0.0206	0.0936
	PS130	0.996	518	0.0114	0.1573
4-CP	PS100	0.998	364	0.0877	0.0175
	PS110	0.994	520	0.0283	0.0522
	PS130	0.994	664	0.0321	0.0463

[a] $R_L = 1/[1 + (K_L C_0)]$.

ues in this study were 38%, 41%, 53%, 68%, 71%, and 79%, uniformly distributed over the middle range of various adsorption systems of dyes on various activated carbons. The q_{mon} values at the top $K_L y_i$ values were 53%, 38%, 71%, and 79% of the adsorption of dyes on the activated carbons of this work; the highest to fourth highest. The above comparisons show that the carbons in this study had both a very high adsorption capacity and a good adsorption performance on dyes.

The Langmuir equation constants of 10 adsorption systems of phenols on various activated carbons reported in literature have been collected in Table 5 and compared with those of this work, the sequence is in the order of the $K_L y_i$ values. The top $K_L y_i$ values of 4-CP in this work were 6%, 19%, and 31%, distributed over the top range of phenols adsorption. The q_{mon} values at the top $K_L y_i$ values were 19%, 31%, and 6% of the 4-CP adsorption, respectively, the second, third, and fifth highest. The above comparisons show that the adsorption capacity and $K_L y_i$ value of 4-CP on the activated carbons in this study were higher than literature. The top $K_L y_i$ values of the phenol adsorption were, respectively, 25%, 50%, and 81%, uniformly distributed over the middle range of the phenols adsorption systems. The q_{mon} values at the top $K_L y_i$ values were 81%, 50%, and 25%, respectively, the fourth, sixth, and ninth highest. The above comparisons show that the adsorption capacity and $K_L y_i$ values of phenol on the activated carbons in this work were in the middle region.

Table 4
Langmuir equation constants of adsorption of dyes on various activated carbons reported in the literature and this work

Dyes	Activated carbon	q_{mon} (g/kg)	K_L (m^3/g)	y_i (g/m^3)	$K_L y_i$	Refs.	Top % of $K_L y_i$
AR151	CBDA	208	0.738	264	195	[10]	3
MS-300	GAC	309	0.369	500	185	[11]	6
BB9	PKSAC	333	0.227	700	159	[12]	9
AR151	CP	169	0.628	223	140	[10]	12
MB	PAC2	345	0.150	800	120	[13]	15
AY117	F400	186	0.400	250	100	[14]	18
MG-400	GAC	159	0.366	200	73	[11]	21
AB80	F400	171	0.260	240	62	[14]	24
RR241	AC4	246	0.061	1000	61	[15]	26
AB113	AC4	345	0.058	1000	58	[15]	29
BR22	kudzu	178	0.055	1000	55	[16]	32
AB74	ADWIC	143	0.191	250	48	[17]	35
MB	PS110	581	0.058	800	46	This work	38
MB	PS100	327	0.056	800	45	This work	41
AY23	ADWIC	57	0.171	250	43	[17]	44
MB	CS700	261	0.091	370	34	[18]	47
AR114	F400	104	0.150	200	30	[14]	50
MB	PS130	883	0.037	800	30	This work	53
AR73	ADWIC	230	0.087	250	22	[17]	56
MB	S800/30	302	0.0023	8529	19	[19]	59
MB	CP55	345	0.044	370	16	[18]	62
AY36	SDC	184	0.01	1000	10	[20]	65
AB74	PS100	102	0.024	400	9.6	This work	68
AB74	PS130	521	0.023	400	9.2	This work	71
Malachite G	BFA	170	0.148	50	7.4	[21]	74
BB1	AC	404	0.017	400	6.8	[22]	76
AB74	PS110	456	0.015	400	6.0	This work	79
BV3	AC	244	0.017	300	5.1	[22]	82
BR9	AC	127	0.012	250	3.0	[22]	85
AY36	RHC	87	0.002	1000	2.0	[20]	88
BR9	AC	303	0.004	300	1.2	[23]	91
BY21	kudzu	380	0.0008	1000	0.8	[16]	94
AB	FSM-16	55	0.008	100	0.8	[24]	97
RB5	PAC	59	0.109	5	0.55	[25]	100

Table 5
Langmuir equation constant values of the adsorption systems of phenols on activated carbons reported in literature

Adsorbate	Adsorbent	q_{mon} (g/kg)	K_L (m^3/g)	y_i (g/m^3)	$K_L y_i$	Refs.	Top % of $K_L y_i$
4-CP	PS100	364	0.0877	642	56	This work	6
2,4,6-TCP	CSAC	122	0.048	500	24	[26]	13
4-CP	PS130	664	0.0321	642	21	This work	19
Phenol	PS100	251	0.0428	470	20	This work	25
4-CP	PS110	520	0.0283	642	18	This work	31
4-CP	CSAC	73	0.019	700	13	[26]	38
Phenol	Commercial	50	0.110	100	11	[27]	44
Phenol	PS110	349	0.0206	470	9.7	This work	50
Phenol	Eurocab YAO	867	0.0089	940	8.4	[28]	56
4- NP	S800/30	328	0.0012	6910	8.0	[19]	63
Phenol	F-400	205	0.042	180	7.6	[29]	69
Phenol	S800/30	235	0.0013	4700	6.2	[19]	75
Phenol	PS130	518	0.0114	470	5.4	This work	81
2-CP	Norit PKDA	270	0.026	200	5.2	[30]	88
Phenol	Activated 850/5	178	0.0037	940	3.5	[28]	94
Phenol	ACAS	126	0.00094	200	0.2	[31]	100

4.3. Design and operation of a countercurrent two-stage adsorption system

Though, in theory, countercurrent two-stage adsorption operation can save significant amounts of adsorbent, its adsorption process had not yet been investigated. A countercurrent two-stage system for batch operation was designed in this study as shown in Fig. 8. It was composed of an adsorption agitation tank, a middle tank, and a centrifugal filter. The operation procedures and calculations were as follows:

1. First, draw up an operation process calculation table as shown in Table 6. The adsorptions of four solutes on PS110 were used as examples.
2. Fill in the known values of Langmuir constant K_L and q_{mon}, and operation conditions of the adsorption process: initial concentration (C_i) and final concentration (C_f) at steady state.

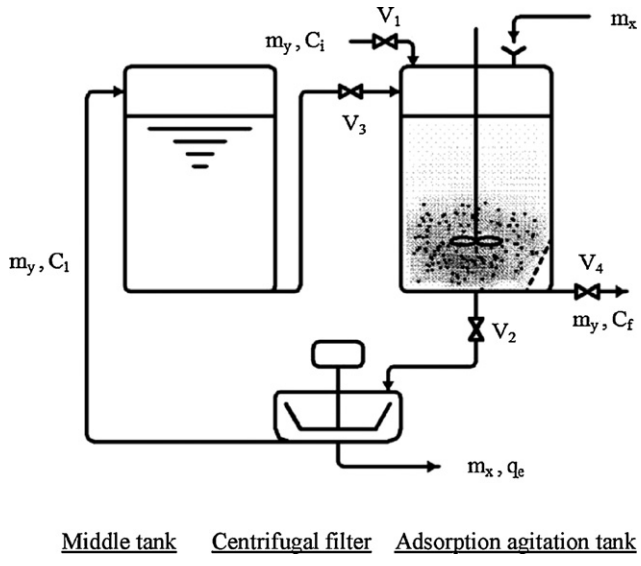

Fig. 8. Design of a countercurrent two-stage adsorption system.

3. Eq. (13) is rewritten as

$$\frac{C_2 - C_f}{C_i - C_f} = \left(\frac{C_f}{C_2}\right)\left[\frac{(1 + K_L C_2)}{(1 + K_L C_f)}\right] \tag{26}$$

The middle concentration (C_2) at steady state is obtained from Eq. (26).

4. Adsorbent consumption is obtained from the Langmuir equation as in Eq. (27)

$$\frac{M_{xs}}{C_0 - C_e} = \frac{K_L q_{mon} C_e}{1 + K_L C_e} \tag{27}$$

The adsorbent mass (M_{xs}) of the single stage one is obtained by substituting, respectively, C_e and C_0 in Eq. (27) with C_f and C_i in Table 6, and the adsorbent mass ($M_{xd,Count.}$) of the countercurrent two-stage one is calculated from Eq. (28), which is obtained by rearranging Eq. (14).

$$M_{xd,Count.} = M_{xs}\left[\frac{C_i - C_f}{C_2 - C_f}\right] \tag{28}$$

Table 6 shows that the values of M_{xs} (adsorbent consumption) were from 4.29 to 15.25 kg/m^3, while those of $M_{xd,Count.}$ were significantly lower, from 1.45 to 2.22 kg/m^3.

5. q_e value at steady state of the countercurrent two-stage one is then be calculated from Eq. (29)

$$q_e = \frac{M_{xd,Count.}}{C_i - C_f} \tag{29}$$

6. After the upper eight lines of basic data are filled in Table 6, proceed to the countercurrent two-stage operations and calculations. First, add the solution with mass M_y and concentration C_i and virgin adsorbent with mass $M_{xd,Count.}$ to the agitation tank. The mixture is stirred and after equilibrium is reached, valve V2 is opened, then, adsorbent and solution are separated with the filter. The separated solution and adsorbed amount in adsorbent are denoted, respectively, as 1st C_2 and 1st q_e. Then, the separated solution is pumped into the middle tank. The value of 1st C_2 is calculated

Table 6
Adsorbent consumption ratio of PS110 in the countercurrent two-stage process

	Solutes	MB	AB74	Phenol	4-CP
Basic data and operation conditions	K_L (m^3/g)	0.0583	0.0154	0.0206	0.0283
	q_{mon} (g/kg)	581	456	349	520
	C_i (g/m^3)	800	400	470	642
	C_f (g/m^3) at S.S.	8.0	4.0	4.7	6.42
Calculation values	C_2 (g/m^3) at S.S.	276	54.4	73.1	131
	q_e (g/kg) at S.S.	546	204	210	408
	M_{xs} (kg/m^3)	4.286	15.25	15.10	7.950
	$M_{xd,Count.}$ (kg/m^3)	1.450	1.940	2.220	1.558
1st batch	1st C_2 (g/m^3)	91.1	43.8	55.9	80.0
	1st q_e (g/kg)	489	184	187	361
	1st C_f (g/m^3)	2.02	3.13	3.52	3.67
2nd batch	2nd C_2(g/m^3)	139	51.1	69.6	108
	2nd q_e (g/kg)	517	201	206	392
	2nd C_f (g/m^3)	3.29	3.68	4.61	5.14
3rd batch	3rd C_2 (g/m^3)	170	52.4	72.1	119.5
	3rd q_e (g/kg)	528.1	203.6	208.5	401.4
	3rd C_f (g/m^3)	4.20	3.78	4.62	5.80

from Eq. (27) with M_x and C_0 substituted, respectively, by $M_{xd,Count.}$ and C_i, and the obtained C_e is 1st C_2. The 1st q_e is obtained from Eq. (29) with C_f substituted by 1st C_2. This 1st q_e value is slightly lower than the q_e value at steady state in Table 6.

7. The solution with concentration 1st C_2 in the middle tank is sent back to the agitation tank with virgin adsorbent with mass $M_{xd,Count.}$ The mixture is stirred. After equilibrium is reached, valve V4 is opened, and the solution with concentration 1st C_f flows out. In front of valve V4, a slant filter is installed to avoid loss of adsorbent. Then, 1st C_f is calculated from Eq. (27) with M_x and C_0 in Eq. (27) being substituted, respectively, by $M_{xd,Count.}$ and 1st C_2, and the obtained equilibrium concentration is 1st C_f. This value is slightly less than the C_f value at the steady state in Table 6.
8. Valve V4 is shut, and valve V1 is opened. A solution with mass M_y and concentration C_i is pumped into the agitation tank and mixed with the remaining adsorbent. After equilibrium is reached, the mixture is separated with the filter, and the separated solution is pumped into the middle tank. The concentration and adsorbed amount of adsorbent are denoted, respectively, as 2nd C_2 and 2nd q_e. Then, 2nd C_2 is calculated from the following Eq. (30):

$$\left[\frac{C_i - 2\text{nd}\,C_2}{M_{xd,Count.}}\right] + \left[\frac{1\text{st}\,C_2 - 1\text{st}\,C_f}{M_{xd,Count.}}\right] = \frac{K_L q_{mon} 2\text{nd}\,C_2}{1 + K_L 2\text{nd}\,C_2} \quad (30)$$

The first term on the left side of Eq. (30) is the adsorbed amount of the first stage of the 2nd batch, and the second term is the adsorbed amount of the second stage of the 1st batch. The 2nd q_e value is the sum of the two terms on the left side of Eq. (30). The 2nd q_e value in Table 6 gradually approaches q_e value at steady state.

9. The solution with concentration 2nd C_2 in the middle tank is pumped back to the agitation tank, and a virgin adsorbent with mass ($M_{xd,Count}$) is added and mixed. After equilibrium is reached, valve V4 is opened, and the solution with concentration 2nd C_f flows out. The 2nd C_f value is calculated from Eq. (27) with M_x and C_2 being substituted, respectively, with $M_{xd,Count.}$ and 2nd C_2 and the obtained equilibrium concentration is 2nd C_f. The 2nd C_f value in Table 6 is closer to C_f at steady state.
10. The first stage of the 3rd batch operation repeats procedure 8 and the second stage repeats procedure 9. The obtained 3rd q_e and 3rd C_f values are close, respectively, to q_e and C_f at steady state. So, after three batches, they can be estimated with q_e and C_f at steady state.
11. If the original single stage adsorption operation is converted to the countercurrent two-stage operation, only the addition of one middle tank is needed saving at least 66% to 87% on adsorbent consumption.

5. Conclusions

The liquid–solid phase equilibrium relationship was expressed with the Langmuir equation in this study. The equilibrium-stage principle was employed to analyze the countercurrent multi-stage adsorption process. Single-, two-, three-, and infinite-stage adsorption operations were done by adjusting the slope of the operating line as graphically explained. The required adsorbent ratio of countercurrent multi-stage adsorption operation with various stages can be obtained from the slopes of the operating line. The Langmuir parameter ($K_L y_i$) was varied to obtain the required adsorbent amount and help determining the optimum number of stages for the countercurrent multi-stage operation and adsorbent reduction in the adsorption systems.

In this study, Pistachio shell activated carbon was prepared by the two-step activation process KOH etching followed by CO_2 gasification. Activated carbons (denoted as PS100, PS110, and PS130) with a BET surface area of 1013, 1398, and 1919 m^2/g were obtained after CO_2 gasification times of 0, 10, and 30 min. Isotherm equilibrium adsorptions of four adsorbates on these activated carbons were investigated. The isotherm curve types of the various adsorbates were quite different, and good linear relationship with the Langmuir isotherm equation was obtained. The Langmuir parameter $K_L y_i$ and q_{mon} values of various activated carbons reported in the literature were compared with those of the activated carbons in this study for the adsorption systems of dyes on activated carbons. The $K_L y_i$ values of the activated carbon in this work were uniformly distributed over the middle region, while the q_{mon} values were higher than those of other activated carbons. For the adsorption systems of phenols on activated carbons, the $K_L y_i$ and q_{mon} values of the adsorption systems of 4-CP on the activated carbons in this work were all in the top region, and the $K_L y_i$ and q_{mon} values of the adsorption systems of phenol were in the middle region.

This paper proposes a countercurrent two-stage adsorption system design. The adsorption systems of four adsorbents on activated PS110 were employed as practical examples for evaluating concentration variations and the adsorbent amounts of the system during operation. By simply adding a middle tank to the traditional single batch adsorption system it can be converted into a countercurrent two-stage adsorption system saving 66% to 87% on adsorbent consumption.

Acknowledgment

Financial support of this work by the National Science Council of the Republic of China under contract no. NSC 95-2214-E-239-001 is gratefully acknowledged.

References

[1] A.J. deRosset, R.W. Neuzil, D.J. Korous, Liquid column chromatography as a predictive tool for continuous countercurrent adsorptive separations, Ind. Eng. Process Des. Dev. 15 (1976) 261–266.
[2] J. Vanderschuren, The plate efficiency of multistage fluidized-bed adsorbers, Chem. Eng. J. 21 (1981) 1–9.
[3] D.M. Ruthven, The axial dispersed plug flow model for continuous countercurrent adsorbers, Can J. Chem. Eng. 61 (1983) 881–883.
[4] C.C. Hu, C.C. Wang, F.C. Wu, R.L. Tseng, Characterization of Pistachio shell-derived carbons activated by a combination of KOH and CO_2 for electric double-layer capacitors, Electrochim. Acta 52 (2007) 2498–2505.
[5] R.L. Tseng, F.C. Wu, R.S. Juang, Liquid-phase adsorption of dyes and phenols using pinewood-based activated carbons, Carbon 41 (2003) 487–495.
[6] F.C. Wu, R.L. Tseng, R.S. Juang, Preparation of highly microporous carbons from fir wood by KOH activation for adsorption of dyes and phenols from water, Sep. Purif. Technol. 47 (2005) 10–19.
[7] K. Kinoshita, Carbon Electrochemical and Physicochemical Properties, John-Wiley & Sons, New York, 1988.
[8] P.Z. Cheng, H. Teng, Electrochemical responses from surface oxide present on HNO_3 treated carbons, Carbon 41 (2003) 2057–2063.
[9] Y. Otake, R.G. Jenkins, Characterization of oxygen-containing surface complexes created on a microporous carbon by air and nitric acid treatment, Carbon 31 (1993) 109–121.
[10] P. Baskaralingam, M. Pulikesi, V. Ramamurthi, S. Sivanesan, Equilibrium studies for the adsorption of acid dyes onto modified hectorite, J. Hazard. Mater. B 136 (2006) 989–992.
[11] V. Meshko, L. Markovska, M. Mincheva, A.E. Rodrigues, Adsorption of basic dyes on granular activated carbon and natural zeolite, Water Res. 35 (2001) 3357–3366.
[12] A. Jumasiah, T.G. Chuah, J. Gimbon, T.S.Y. Choong, I. Azni, Adsorption of basic dye onto palm kernel shell activated carbon: sorption equilibrium and kinetics studies, Desalination 186 (2005) 57–64.
[13] E.N. El Qada, S.J. Allen, G.M. Walker, Adsorption of methylene blue onto activated carbon produced from steam activated bituminous coal: a study of equilibrium adsorption isotherm, Chem. Eng. J. 124 (2006) 103–110.
[14] K.K.H. Choy, J.F. Porter, G. Mckay, Intraparticle diffusion in single and mulyicomponent acid dye adsorption from wastewater onto carbon, Chem. Eng. J. 103 (2004) 133–145.
[15] P.C.C. Faria, J.J.M. Órfão, M.F.R. Pereira, Adsorption of anionic and cationic dyes on activated carbons with different surface chemistries, Water Res. 38 (2004) 2043–2052.
[16] S.J. Allen, Q. Gan, R. Matthews, P.A. Johnson, Comparison of optimized isotherm models for basic dye adsorption by kudzu, Bioresour. Technol. 88 (2003) 143–152.
[17] A.A. Attia, W.E. Rashwan, S.A. Khedr, Capacity of activated carbon in the removal of acid dyes subsequent to its thermal treatment, Dyes Pigments 69 (2006) 128–136.
[18] A-N.A. El-Hendawy, Influence of HNO_3 oxidation on the structure and adsorptive properties of corncob-based activated carbon, Carbon 41 (2003) 713–722.
[19] A.M. Warhurst, G.L. McConnachie, S.J.T. Pollard, Characterization and applications of activated carbon produced from moringa oleifera seed husks by single-step steam pyrolysis, Water Res. 31 (4) (1997) 759–766.
[20] P.K. Malik, Use of activated carbons prepared from sawdust and rice-husk for adsorption of acid dyes: a case study Acid Yellow 36, Dyes Pigments 56 (2003) 239–249.
[21] I.D. Mall, V.C. Srivastava, N.K. Agarwal, I.M. Mishra, Adsorptive removal of malachite green dye from aqueous solution by bagasse fly ash and activated carbon-kinetic study and equilibrium isotherm analyses, Colloids Surf. A 264 (2005) 17–28.
[22] K.V. Kumar, S. Sivanesan, Isotherm parameters for basic dyes onto activated carbon: comparison of linear and non-linear method, J. Hazard. Mater. B 129 (2006) 147–150.
[23] V.K. Gupta, I. Ali, D. Suhas, Mohan, Equilibrium uptake and sorption dynamics for the removal of a basic dye (basic red) using low-cost adsorbents, J. Colloid Interface Sci. 265 (2003) 257–264.
[24] M.M. Mohamed, Acid dye removal: comparison of surfactant-modified mesoporous FSM-16 with activated carbon derived from rice husk, J. Colloid Interface Sci. 272 (2004) 28–34.
[25] Z. Eren, F.N. Acar, Adsorption of reactive black 5 an aqueous solution: equilibrium and kinetic studies, Desalination 194 (2006) 1–10.
[26] M. Radhika, K. Palanivelu, Adsorptive removal of chlorophenols from aqueous solution by cost adsorbent-Kinetics and isotherm analysis, J. Hazard. Mater. B138 (2006) 116–124.
[27] B. Ozkaya, Adsorption and desorption of phenol on activated carbon and a comparison of isotherm models, J. Hazard. Mater. B 129 (2006) 158–163.
[28] S.J.T. Pollard, F.E. Thompson, G.L. McConnachie, Microporous carbons from moringa oleifera husks for water purification in less developed countries, Water Res. 29 (1) (1995) 337–347.
[29] N. Roostaei, H. Tezel, Removal of phenol from aqueous solutions by adsorption, J. Environ. Manage. 70 (2004) 157–164.
[30] O. Aktas, F. Cecen, Adsorption, Desorption and bioregeneration in the treatment of 2-chlorophenol with activated carbon, J. Hazard. Mater. B 141 (2007) 769–777.
[31] A. Aygun, S. Yenisoy-Karakas, I. Duman, Production of granular activated carbon from fruit stones and nutshells and evaluation of their physical, chemical and adsorption properties, Micropor. Mesoporo. Mater. 66 (2003) 189–195.